World Academy of Science, Engineering and Technology
International Journal of Physical and Mathematical Sciences
Vol:8, No:1, 2014

Coupled Galerkin-DQ Approach for the Transient Analysis of Dam-Reservoir Interaction

S. A. Eftekhari

***Abstract*—**In this paper, a numerical algorithm using a coupled Galerkin-Differential Quadrature (DQ) method is proposed for the solution of dam-reservoir interaction problem. The governing differential equation of motion of the dam structure is discretized by the Galerkin method and the DQM is used to discretize the fluid domain. The resulting systems of ordinary differential equations are then solved by the Newmark time integration scheme. The mixed scheme combines the simplicity of the Galerkin method and high accuracy and efficiency of the DQ method. Its accuracy and efficiency are demonstrated by comparing the calculated results with those of the existing literature. It is shown that highly accurate results can be obtained using a small number of Galerkin terms and DQM sampling points. The technique presented in this investigation is general and can be used to solve various fluid-structure interaction problems.

***Keywords*—**Dam-reservoir system, Differential quadrature method, Fluid-structure interaction, Galerkin method, Integral quadrature method.

I. Introduction

THE dynamic response of dam-reservoir systems subjected to earthquake excitation has long been an interesting topic in the field of civil engineering. In early studies, an added mass approach was used where the water incompressibility and rigid structure were assumed [1]-[4]. This is the simplest form of treating the dam-reservoir problem. Some simplified approaches are also available in which fluid-structure interaction is studied in a decoupled manner. In these approaches, the fluid response is first obtained assuming the structure to be rigid and the resulting pressure field is imposed on the structure to obtain the structural response. However, when coupled modes are excited, these approaches may lead to inaccurate results [5]. Thus it is necessary to study the fluid-structure interaction in a coupled manner considering the flexibility of the structure.

Two kinds of methods, i.e., analytical and numerical methods, have been widely used to tackle the problem. As analytical methods are often limited to simple dam-reservoir problems, many researchers have resorted to various numerical methods [6]-[24]. Among them, the Finite Element Method (FEM) is one of the most popular numerical methods used by many researchers to handle the problem. Conventionally, the structure and the fluid domain are treated as two separate systems and discretized by the FEM. The resulting systems of ordinary differential equations are then solved separately or simultaneously using various time integration schemes. Although the FEM is especially powerful due to its versatility in the spatial discretization, the number of unknowns involved and the amount of input data are very large in the FEM. On the other hand, in the finite element analysis of such problems, difficulties arise mainly because of the large extent of the fluid domain where fluid is practically unbounded. To solve this problem, the unbounded domain should be truncated at a certain distance away from the structure. Clearly, when a low-order FEM (say *h*-version FEM) is used for the solution of such fluid-structure interaction problems, many calculations should be done to accurately predict the location of the truncated boundary. Therefore, to accurately predict the location of the truncated boundary and to reduce the computational time, higher-order numerical methods should be used to model the fluid-structure interaction problems. To tackle this limitation, one may use the FEM with higher-order polynomials (i.e., the *p*-version FEM). The *p*-version FEM employs a fixed mesh, and the convergence is sought by increasing the degrees of the elements. It is well-known that the convergence of the *p*-version FEM is more rapid than that of the *h*-version FEM by using the same number of degrees of freedom (DOF). However, the calculation of the stiffness and mass matrices is expensive in the *p*-version FEM, and the cost will increase dramatically when using a large number of DOFs.

To overcome the difficulties of the FEM in modeling such types of problems, one may use the boundary element method (BEM) or a combination of FEM and BEM to discretize the problem domain. When BEM is applied to fluid-structure interaction problems with unbounded fluid domains, then no artificial or truncated boundaries are introduced because the analytic fundamental solutions of BEM satisfy the infinite boundary conditions of the problem. However, because of the presence of the convolution integrals and singularity of the kernels of the formulation, the BEM requires large storage space and computational time for the numerical integration of the kernels. Besides, the use of BEM requires the solution of an unbounded matrix. Therefore, the BEM does not seem to possess any significant advantage over the FEM.

To overcome the above mentioned difficulties, this paper presents a simple mixed method in which the number of unknowns is substantially reduced. In this method, the Galerkin method is applied for the structural part, whereas the DQM is used for the fluid domain. The proposed mixed method combines the simplicity of the Galerkin method and high accuracy and efficiency of the DQM. Its accuracy and efficiency are demonstrated by comparing the calculated

S. A. Eftekhari is with the Young Researchers and Elite Club, Karaj Branch, Islamic Azad University, Karaj, Iran (phone: +98-919-4618599; e-mail: aboozar.eftekhari@gmail.com).

results with those of the existing literature.

II. Governing Equations and Boundary Conditions

Fig. 1 shows a variable thickness dam-structure of height L in contact with a fluid of unbounded domain. The dam-structure is assumed to behave as a cantilever beam of variable thickness. The governing differential equation for the transverse vibration of the dam-structure is [9]

$$\frac{\partial^2}{\partial z^2}\left(EI(z)\frac{\partial^2 w(z,t)}{\partial z^2}\right)+\rho_s A(z)\frac{\partial^2 w(z,t)}{\partial t^2}=-\rho_s A(z)a_g(t)-p(x=0,z,t) \quad (1)$$

where E is elastic modulus, I is the moment inertia of the structure, $w(z,t)$ is the displacement of the structure relative to the ground in the x-direction,ρ_s is the density of the structure, $A(z)$ is the cross-sectional area of the structure, $a_g(t)$ is the ground acceleration and p is the hydrodynamic pressure. The boundary conditions for the structure are as follows:

$$w|_{z=0}=\frac{\partial w}{\partial z}\Big|_{z=0}=\left(EI(z)\frac{\partial^2 w(z,t)}{\partial z^2}\right)\Big|_{z=L}=\frac{\partial}{\partial z}\left(EI(z)\frac{\partial^2 w(z,t)}{\partial z^2}\right)\Big|_{z=L}=0 \quad (2)$$

The hydrodynamic pressure in the fluid domain of the structure-reservoir system is assumed to be governed by the pressure wave equation [9]

$$\nabla^2 p(x,z,t)=\frac{1}{C^2}\frac{\partial^2 p(x,z,t)}{\partial t^2} \quad (3)$$

where $\nabla^2=\frac{\partial^2}{\partial x^2}+\frac{\partial^2}{\partial z^2}$, $p(x,z,t)$ is the hydrodynamic pressure and C is the velocity of sound in fluid.

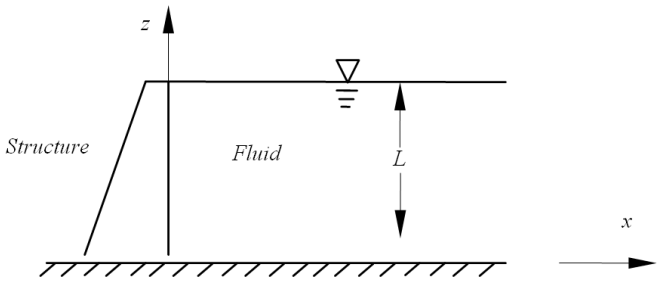

Fig. 1 Fluid-structure system

The boundary conditions for the fluid are as follows:

$$\frac{\partial p}{\partial x}\Big|_{x=0}=-\rho_f\left(a_g(t)+\ddot{w}(z,t)\right) \quad (4)$$

$$\frac{\partial p}{\partial z}\Big|_{z=0}=p|_{z=L}=p|_{x\to\infty}=0 \quad (5)$$

whereρ_f is the density of the fluid. It is noted that the dam-reservoir interaction problem is defined on an unbounded domain ($0\le x\le\infty$, $0\le z\le L$) and the position of the far boundary ($x=x_\infty$) is not known a priori. Thus, the location of the far boundary must also be determined as a part of solutions.

Assuming that the dam and reservoir are initially at rest, the initial conditions are:

$$w|_{t=0}=\frac{\partial w}{\partial t}\Big|_{t=0}=p|_{t=0}=\frac{\partial p}{\partial t}\Big|_{t=0}=0 \quad (6)$$

The problem at hand in to determine the transient responses of the structure and the fluid subjected to ground motion and boundary conditions (2), (4), and(5). In this paper a mixed Galerkin-DQM will be presented to solve the problem. The Galerkin method and the DQM will be separately applied to (1) and (3). The resulting coupled ordinary differential equations will then be solved using the Newmark time integration scheme. The details will be given in next sections.

III. Differential Quadrature Method

Let $f(x,z,t)$ be a solution of a partial differential equation, $z_1,z_2,\dots,z_n$ be a set of sampling points in the z-direction and $x_1,x_2,\dots,x_m$ be that in the x-direction. According to the DQM, the first-order derivative $f_{,z}$ at a sample point (x,z_i,t) can be expressed by the quadrature rules as [25]

$$f_{,z}(x,z_i,t)=\sum_{j=1}^{n}A_{ij}^{(1)}f\left(x,z_j,t\right) \quad (7)$$

where $A_{ij}^{(1)}$ are the first-order z-derivative weighting coefficients associated with the $z=z_i$ point. Equation (7) can also be written for all values of z_i ($i=1,2,\dots,n$) in matrix notation as

$$\{f_{,z}\}=[A^{(1)}]\{f\} \quad (8)$$

where

$$\{f_{,z}\}=[f_{,z}(x,z_1,t)\quad f_{,z}(x,z_2,t)\quad\dots\quad f_{,z}(x,z_n,t)]^T \quad (9)$$

$$\{f\}=[f(x,z_1,t)\quad f(x,z_2,t)\quad\dots\quad f(x,z_n,t)]^T \quad (10)$$

Now, using the quadrature rule, the first-order derivative of the vector $\{f\}$ with respect to the variable x at a sample point $x=x_i$ can be expressed as [26]-[31]:

$$\{f_{,x}(x_i,t)\}=\sum_{j=1}^{m}B_{ij}^{(1)}\{f(x_j,t)\},\qquad j=1,2,\dots,m \quad (11)$$

where$B_{ij}^{(1)}$ are the first-order x-derivative weighting coefficients associated with the $x=x_i$ point, and

$$\{f_{,x}(x_i,t)\}=[f_{,x}(x_i,z_1,t)\quad f_{,x}(x_i,z_2,t)\quad\dots\quad f_{,x}(x_i,z_n,t)]^T \quad (12)$$

$$\{f(x_i,t)\}=[f(x_i,z_1,t)\quad f(x_i,z_2,t)\quad\dots\quad f(x_i,z_n,t)]^T \quad (13)$$

$A_{ij}^{(1)}$and$B_{ij}^{(1)}$ are given by [25]:

$$A_{ij}^{(1)}=\begin{cases}\dfrac{M^{(1)}(z_i)}{(z_i-z_j)M^{(1)}(z_j)} & i\ne j,\quad i,j=1,2,\dots,n\\ -\sum_{k=1,k\ne i}^{n}A_{ik}^{(1)} & i=j,\quad i=1,2,\dots,n\end{cases} \quad (14)$$

$$B_{ij}^{(1)} = \begin{cases} \frac{M^{(1)}(x_i)}{(x_i - x_j)M^{(1)}(x_j)} & i \neq j, \quad i,j = 1,2,\dots,m \\ -\sum_{k=1,k\neq i}^{m} B_{ik}^{(1)} & i = j, \quad i = 1,2,\dots,m \end{cases} \tag{15}$$

where$M^{(1)}(z)$ and $M^{(1)}(x)$ are defined as

$$M^{(1)}(z_i) = \prod_{j=1,j\neq i}^{n}(z_i - z_j), \;\; M^{(1)}(x_i) = \prod_{j=1,j\neq i}^{m}(x_i - x_j) \tag{16}$$

The weighting coefficients of the second-order derivatives may be obtained through the following relationships [32]

$$A_{ij}^{(2)} = \begin{cases} 2A_{ij}^{(1)}\left[A_{ii}^{(1)} - \frac{1}{(z_i - z_j)}\right] & i \neq j, \quad i,j = 1,2,\dots,n \\ -\sum_{k=1,k\neq i}^{n} A_{ik}^{(2)} & i = j, \quad i = 1,2,\dots,n \end{cases} \tag{17}$$

$$B_{ij}^{(2)} = \begin{cases} 2B_{ij}^{(1)}\left[B_{ii}^{(1)} - \frac{1}{(x_i - x_j)}\right] & i \neq j, \quad i,j = 1,2,\dots,m \\ -\sum_{k=1,k\neq i}^{m} B_{ik}^{(2)} & i = j, \quad i = 1,2,\dots,m \end{cases} \tag{18}$$

In this study, the sampling points are taken nonuniformly spaced and are given by the following equations

$$\begin{aligned} &z_1 = 0,\ z_2 = \delta \times L \\ &z_i = L/2\left[1 - \cos\left(\tfrac{(i-2)\pi}{n-3}\right)\right], \quad i = 3,4,\dots,n-2 \\ &z_{n-1} = (1-\delta)\times L,\ z_n = L \end{aligned} \tag{19}$$

$$\begin{aligned} &x_1 = 0,\ x_2 = \delta \times x_\infty \\ &x_i = x_\infty/2\left[1 - \cos\left(\tfrac{(i-2)\pi}{m-3}\right)\right], \quad i = 3,4,\dots,m-2 \\ &x_{m-1} = (1-\delta)\times x_\infty,\ x_m = x_\infty \end{aligned} \tag{20}$$

whereδ is a parameter that shows the closeness between adjacent boundary points and the boundary points. Moreover, L and x_∞ are problem boundaries in z- and x-directions, respectively. It should be pointed out that the δ-technique as proposed in [25] is not used in this paper (i.e., the above sampling points are only used to construct the weighting coefficients). In all computation presented in this paper, $\delta = 10^{-3}$ is taken.

IV. Discretization of Spatial Partial Derivatives

A. Fluid Domain

In this section the DQM will be used to discretize the fluid domain. A simple technique will also be presented to exactly implement the boundary conditions of the fluid domain.

Satisfying (3) at any sample point $z = z_i$, one has

$$p_{,xx}(x,z_i,t) + p_{,zz}(x,z_i,t) = \tfrac{1}{C^2}p_{,tt}(x,z_i,t),\ i = 1,2,\dots,n \tag{21}$$

where a subscript comma denotes differentiation. Substituting the quadrature rule, given in (7), into (21) and implementing the boundary conditions of the fluid domain in z-direction gives

$$[I^z]\{p_{,xx}\} + [\bar{A}]^{(2)}\{p\} = \tfrac{1}{C^2}[I^z]\{p_{,tt}\} \tag{22}$$

where

$$[I^z] = \begin{bmatrix} 0 & 0 & . & . & . & 0 \\ 0 & 1 & 0 & . & . & 0 \\ . & 0 & . & 0 & . & 0 \\ . & . & 0 & . & 0 & 0 \\ . & . & . & 0 & . & 0 \\ 0 & 0 & . & . & 0 & 1 \end{bmatrix}_{(n-1)\times(n-1)} \tag{23}$$

$$[\bar{A}]^{(2)} = \begin{bmatrix} A_{11}^{(1)} & A_{12}^{(1)} & . & . & . & A_{1,n-1}^{(1)} \\ A_{21}^{(2)} & A_{22}^{(2)} & . & . & . & A_{2,n-1}^{(2)} \\ A_{31}^{(2)} & A_{32}^{(2)} & . & . & . & A_{3,n-1}^{(2)} \\ . & . & . & . & . & . \\ . & . & . & . & . & . \\ A_{n-1,1}^{(2)} & A_{n-1,2}^{(2)} & . & . & . & A_{n-1,n-1}^{(2)} \end{bmatrix}_{(n-1)\times(n-1)} \tag{24}$$

$$\{p_{,xx}\} = [p_{,xx}(x,z_1,t) \quad p_{,xx}(x,z_2,t) \quad \dots \quad p_{,xx}(x,z_{n-1},t)]^T \tag{25}$$

$$\{p\} = [p(x,z_1,t) \quad p(x,z_2,t) \quad \dots \quad p(x,z_{n-1},t)]^T \tag{26}$$

$$\{p_{,tt}\} = [p_{,tt}(x,z_1,t) \quad p_{,tt}(x,z_2,t) \quad \dots \quad p_{,tt}(x,z_{n-1},t)]^T \tag{27}$$

Now, Satisfying (22) at any sample point $x = x_i$, one has

$$[I^z]\{p_{,xx}(x_i,t)\} + [\bar{A}]^{(2)}\{p(x_i,t)\} = \tfrac{1}{C^2}[I^z]\{p_{,tt}(x_i,t)\}, i = 1,2,\dots,m \tag{28}$$

Substituting the quadrature rule, given in (11), into (28) gives

$$[I^z]\textstyle\sum_{j=1}^{m} B_{ij}^{(2)}\{p(x_j,t)\} + [\bar{A}]^{(2)}\{p(x_i,t)\} = \tfrac{1}{C^2}[I^z]\{p_{,tt}(x_i,t)\}, i = 1,2,\dots,m \tag{29}$$

Equation (29) can be written in compact form as

$$[K^f]\{\tilde{p}\} = [M^f]\{\ddot{\tilde{p}}\} \tag{30}$$

where the $(n-1)\times(n-1)$ sub-matrices $\left[K_{ij}^f\right]$ and $\left[M_{ij}^f\right]$ $(i,j = 1,2,\dots,m)$ are given by

$$\left[K_{ij}^f\right] = B_{ij}^{(2)}[I^z] + I_{ij}^x[\bar{A}]^{(2)} \tag{31}$$

$$\left[M_{ij}^f\right] = \tfrac{1}{C^2}I_{ij}^x[I^z] \tag{32}$$

and

$$\{\tilde{p}\} = [\{p(x_1,t)\}^T \quad \{p(x_2,t)\}^T \quad \dots \quad \{p(x_m,t)\}^T]^T \tag{33}$$

$$\{\ddot{\tilde{p}}\} = \tfrac{d^2}{dt^2}\{\tilde{p}\} \tag{34}$$

whereI_{ij}^x are the elements of the $m \times m$ identity matrix. Furthermore,$[K^f]$ and $[M^f]$ represent the stiffness and mass matrices of the fluid, respectively.

At this stage, the boundary conditions of the fluid in x-direction should be applied to (30). Using (4), (5) and (11) the quadrature analog of boundary conditions are obtained as

$$\{p_{,x}(x_1,t)\} = \textstyle\sum_{j=1}^{m} B_{1j}^{(1)}\{p(x_j,t)\} == -\rho_f(\{a_g(t)\} + \{\ddot{w}(t)\}) \tag{35}$$

$$\{p(x_m,t)\} = \{0\}_{(n-1)\times 1} \tag{36}$$

where$\{0\}_{(n-1)\times 1}$ is the zero vector of size $(n-1)\times 1$ and

$$\{a_g(t)\} = a_g(t)[1 \quad 1 \quad \dots \quad 1]^T \tag{37}$$

$$\{\ddot{w}(t)\} = [\ddot{w}(z_1,t) \quad \ddot{w}(z_2,t) \quad \dots \quad \ddot{w}(z_{n-1},t)]^T \tag{38}$$

Now substituting the above quadrature analogs into (30) yields:

$$[\bar{K}^f]\{\bar{p}\} = [\bar{M}^f]\{\ddot{\bar{p}}\} + \{F^g\} + \{F^w\} \tag{39}$$

where

$$[\bar{K}^f] = \begin{bmatrix} B_{11}^{(1)}[\bar{I}^z] & B_{12}^{(1)}[\bar{I}^z] & \cdots & B_{1,m-1}^{(1)}[\bar{I}^z] \\ [K_{21}^f] & [K_{22}^f] & \cdots & [K_{2,m-1}^f] \\ [K_{31}^f] & [K_{32}^f] & \cdots & [K_{3,m-1}^f] \\ \vdots & \vdots & \ddots & \vdots \\ [K_{m-1,1}^f] & [K_{m-1,2}^f] & \cdots & [K_{m-1,m-1}^f] \end{bmatrix} \tag{40}$$

$$[\bar{M}^f] = \begin{bmatrix} [0] & [0] & \cdots & [0] \\ [0] & [M_{22}^f] & \cdots & [0] \\ \vdots & \vdots & \ddots & \vdots \\ [0] & [0] & \cdots & [M_{m-1,m-1}^f] \end{bmatrix} \tag{41}$$

$$\{\bar{p}\} = [\{p(x_1,t)\}^T \quad \{p(x_2,t)\}^T \quad \dots \quad \{p(x_{m-1},t)\}^T]^T \tag{42}$$

$$\{\ddot{\bar{p}}\} = \frac{d^2}{dt^2}\{\bar{p}\} \tag{43}$$

$$\{F^g\} = \left[-\rho_f\{a_g(t)\}^T \quad \{0\}^T \quad \{0\}^T \quad \dots \quad \{0\}^T\right]^T \tag{44}$$

$$\{F^w\} = \left[-\rho_f\{\ddot{w}(t)\}^T \quad \{0\}^T \quad \{0\}^T \quad \dots \quad \{0\}^T\right]^T \tag{45}$$

where$[\bar{I}^z]$ and $[0]$ are the identity and zero matrices of size $(n-1)\times(n-1)$, respectively, and $\{0\}$ is the is the zero vector of size $(n-1)\times 1$. Note that the size of matrices $[\bar{K}^f]$ and $[\bar{M}^f]$ is $(n-1)(m-1)\times(n-1)(m-1)$ while the vectors $\{\bar{p}\}$ and $\{\ddot{\bar{p}}\}$ are of order $(n-1)(m-1)\times 1$. Moreover, $\{F^g\}$ is the force vector due to the ground motion and $\{F^w\}$ is that due to the structure motion.

B. Structural Domain

The governing differential equation for the motion of the structure is given in (1). In the Galerkin method, we seek an approximate solution to (1) in the form of a finite series

$$w(z,t) = d_1(t) + d_2(t)z + d_3(t)z^2 + \cdots + d_{N+1}(t)z^N = \sum_{j=1}^{N+1} d_j(t)z^{j-1} \tag{46}$$

where$d_j(t)$ $(j = 1,2,\dots,N+1)$ are unknown coefficients (that are functions of time) and N is the order of approximate functions. It is seen that the displacement of the structure is expressed in a general series form and it does not satisfy the geometric boundary conditions of the structure. To overcome this, we consider a number of grid points in the z-direction on the structure domain and assume each grid point has two degrees of freedom (displacement and slope). Let

$$W_i(t) = \begin{cases} W(z_{(i+1)/2},t) & i = 1,3,5,\dots \\ W_{,z}(z_{i/2},t) & i = 2,4,6,\dots \end{cases} \tag{47}$$

where$W_i(t)$ $(i = 1,3,5,\dots)$ are nodal displacements and $W_i(t)$ $(i = 2,4,6,\dots)$ are nodal slopes. Substituting (47) in (46) gives

$$W(z_{(i+1)/2},t) = \sum_{j=1}^{N+1} d_j(t) z_{(i+1)/2}^{j-1}, \quad i = 1,3,5,\dots \tag{48}$$

$$W_{,z}(z_{i/2},t) = \sum_{j=1}^{N+1}(j-1)d_j(t)z_{i/2}^{j-2}, \quad i = 2,4,6,\dots \tag{49}$$

From (48) and (49) one can express $d_j(t)$ $(j = 1,2,\dots,N+1)$ in terms of nodal variables $W_i(t)$ $(i = 1,2,\dots,N+1)$. By doing so and substituting the result into (46), one obtains

$$w(z,t) = \sum_{j=1}^{N+1} W_j(t)\psi_j(z) \tag{50}$$

where $\psi_j(z)$ are the interpolation functions of degree N. Note that since each node on the structure domain has only two degrees of freedom, the order of interpolation functions (i.e., N) must be an odd number (i.e., $N = 3,5,7,\dots$).

Now, substituting (50) into (1), multiplying both sides of resulting equations by $\psi_i(z)$ and performing the integration over the length of the structure ($0 \le z \le L$), we obtain

$$[M^s]\{\ddot{W}\} + [K^s]\{W\} = \{f^g\} + \{f^p\} \tag{51}$$

where $(i,j = 1,2,\dots,N+1)$

$$M_{ij}^s = \int_0^L \rho_s A(z)\psi_i\psi_j dz \tag{52}$$

$$K_{ij}^s = \int_0^L \psi_i(EI(z)\psi_{j,zz})_{,zz}dz = \left[\psi_i(EI(z)\psi_{j,zz})_{,z}\right]_0^L - \left[\psi_{i,z}(EI(z)\psi_{j,zz})\right]_0^L + \int_0^L EI(z)\psi_{i,zz}\psi_{j,zz}dz \tag{53}$$

$$f_i^g = -\rho_s a_g(t)\int_0^L A(z)\psi_i dz \tag{54}$$

$$f_i^p = -\int_0^L p(x=0,z,t)\psi_i dz \tag{55}$$

$$\{W\} = [W_1 \quad W_2 \quad \dots \quad W_{N+1}]^T \tag{56}$$

$$\{\ddot{W}\} = \frac{d^2}{dt^2}\{W\} \tag{57}$$

where $[M^s]$ and $[K^s]$ are structural mass and stiffness matrices, $\{f^g\}$ and $\{f^p\}$ are load vectors due to ground motion and hydrodynamic pressure of the fluid, respectively, $\{W\}$ and $\{\ddot{W}\}$ are the displacement and acceleration vectors of the nodal values.

At this step of the analysis, the geometric boundary conditions of the structure should be imposed to (51). This can be done simply by deleting the first and second columns and rows of the stiffness and mass matrices and by eliminating the first and second rows of the force vectors. Thus, after implementing the geometric boundary conditions, the size of mass and stiffness matrices is $(N-1)\times(N-1)$ while the displacement and force vectors are of order$(N-1)\times 1$.

V. Solution of Resulting Systems of Ordinary Differential Equations

It can be seen from (39) and (51) that the equations of motions of the fluid and the structures are coupled with each other through the force vectors $\{F^w\}$and $\{f^p\}$. Therefore, it is necessary to describe $\{F^w\}$ in terms of nodal variables and $\{f^p\}$ in terms of pressure values at sampling points.

Using the *integral quadrature rule*, the force vector $\{f^p\}$ can be expressed as

$$\{f^p\} = -[][V]\{p^I\} \tag{58}$$

where

$$[] = \begin{bmatrix} \psi_3(z_1) & \psi_3(z_2) & \cdots & \psi_3(z_{n-1}) \\ \psi_4(z_1) & \psi_4(z_2) & \cdots & \psi_4(z_{n-1}) \\ \vdots & \vdots & \vdots & \vdots \\ \psi_{N+1}(z_1) & \psi_{N+1}(z_2) & \cdots & \psi_{N+1}(z_{n-1}) \end{bmatrix}_{(N-1)\times(n-1)} \tag{59}$$

$$[V] = \begin{bmatrix} V_1 & 0 & \cdots & 0 \\ 0 & V_2 & \cdots & 0 \\ \vdots & \vdots & \ddots & \vdots \\ 0 & 0 & \cdots & V_{n-1} \end{bmatrix}_{(n-1)\times(n-1)} \tag{60}$$

$$\{p^I\} = [p(0,z_1,t) \quad p(0,z_2,t) \quad \dots \quad p(0,z_{n-1},t)]^T = \{p(x_1,t)\} \tag{61}$$

whereV_i $(i = 1,2,\dots,n-1)$ are weights for the *integral quadrature rule* and the vector $\{p^I\} = \{p(x_1,t)\}$ is the interface hydrodynamic pressure.

It can also be easily verified that:

$$\{w(t)\} = \begin{Bmatrix} w(z_1,t) \\ w(z_2,t) \\ w(z_3,t) \\ \vdots \\ w(z_{n-1},t) \end{Bmatrix} = []^T\{W\} \tag{62}$$

and

$$\{\ddot{w}(t)\} = \begin{Bmatrix} \ddot{w}(z_1,t) \\ \ddot{w}(z_2,t) \\ \ddot{w}(z_3,t) \\ \vdots \\ \ddot{w}(z_{n-1},t) \end{Bmatrix} = []^T\{\ddot{W}\} \tag{63}$$

where the vectors $\{W\}$ and $\{\ddot{W}\}$ are nodal displacements and accelerations.Therefore, the governing equations for the motion of the structure and fluid can be rewritten as:

$$[M^s]\{\ddot{W}\} + [K^s]\{W\} = \{f^g\} - [][V]\{p^I\} \tag{64}$$

$$[\bar{K}^f]\{\bar{p}\} = [\bar{M}^f]\{\ddot{\bar{p}}\} + \{F^g\} - \rho_f \begin{Bmatrix} []^T\{\ddot{W}\} \\ \{0\}_{(n-1)\times 1} \\ \{0\}_{(n-1)\times 1} \\ \vdots \\ \{0\}_{(n-1)\times 1} \end{Bmatrix} \tag{65}$$

Combining (64) with (65), one has

$$\begin{bmatrix} -[\bar{M}^f]_{\tilde{n}\tilde{m}\times\tilde{n}\tilde{m}} & [M^*]_{\tilde{n}\tilde{m}\times\tilde{N}} \\ [0]_{\tilde{N}\times\tilde{n}\tilde{m}} & [M^s]_{\tilde{N}\times\tilde{N}} \end{bmatrix} \begin{Bmatrix} \{\ddot{\bar{p}}\}_{\tilde{n}\tilde{m}\times 1} \\ \{\ddot{W}\}_{\tilde{N}\times 1} \end{Bmatrix} + \begin{bmatrix} [\bar{K}^f]_{\tilde{n}\tilde{m}\times\tilde{n}\tilde{m}} & [0]_{\tilde{n}\tilde{m}\times\tilde{N}} \\ [K^*]_{\tilde{N}\times\tilde{n}\tilde{m}} & [K^s]_{\tilde{N}\times\tilde{N}} \end{bmatrix} \begin{Bmatrix} \{\bar{p}\}_{\tilde{n}\tilde{m}\times 1} \\ \{W\}_{\tilde{N}\times 1} \end{Bmatrix} = \begin{Bmatrix} \{F^g\}_{\tilde{n}\tilde{m}\times 1} \\ \{f^g\}_{\tilde{N}\times 1} \end{Bmatrix} \tag{66}$$

where $\tilde{n} = n-1$, $\tilde{m} = m-1$, and $\tilde{N} = N-1$. Furthermore,

$$[M^*] = \begin{bmatrix} \rho_f[]^T \\ [0]_{\tilde{n}\times\tilde{N}} \\ [0]_{\tilde{n}\times\tilde{N}} \\ \vdots \\ [0]_{\tilde{n}\times\tilde{N}} \end{bmatrix}_{\tilde{n}\tilde{m}\times\tilde{N}} \tag{67}$$

$$[K^*] = [[][V] \quad [0]_{\tilde{N}\times\tilde{n}} \quad [0]_{\tilde{N}\times\tilde{n}} \quad \cdots \quad [0]_{\tilde{N}\times\tilde{n}}]_{\tilde{N}\times\tilde{n}\tilde{m}} \tag{68}$$

Equation (66) can be solved using various time integration schemes. In this study, the Newmark method is used to solve the system (66).

VI. Numerical Results

A. Validation of the Proposed Algorithm

To validate the proposed formulation and its implementation, application is made to a numerical example given by Lee and Tsai [9]. The parameters used in this numerical example are as follows:

$$EI = 9.8437 \times 10^{12}\text{Kgm}^2,\ \rho_s A = 3.6 \times 10^4\ \text{Kg/m},$$
$$L = 180\ m,\ \rho_f = 1000\ \text{Kg/m}^3,\ C = 1438.656\ \text{m/s}$$

Lee and Tsai [9] found an analytical solution for the present problem. Thus, we are able to verify the accuracy of the proposed mixed methodology by comparing the calculated results with those of analytical solutions.

First, we assume that the dam-reservoir system is subjected to ramp acceleration defined as [9]:

$$a_g(t) = \begin{cases} 50A_g t, & 0 \le t \le 0.02 \\ A_g, & t \ge 0.02 \end{cases} \tag{69}$$

whereA_g is a constant.

The dynamic responses of the fluid-structure system subjected to ramp acceleration are evaluated for different values of *N*(order of interpolation functions), *n* (number of DQM sampling points in *z*-direction), *m* (number of DQM sampling points in *x*-direction) and x_∞ (location of truncated or far boundary). The Newmark time integration with $\alpha = 0.25$ and $\delta = 0.5$ is used to solve the resulting system of coupled ordinary differential equations [33]. In all

computation, time step $\Delta t = 0.02\ s$ is taken.

Fig. 2 presents the convergence of solutions with respect to the order of interpolation functions (N) for the displacements at top of the structure for empty and full reservoirs. It can be seen that the converging trend of solutions is excellent. It can also be seen that the results converge to their final values using $N = 5$. The solution convergence behavior according to the number of DQM sampling points (n and m) is shown in Fig. 3. A very good convergence behavior is observed. It is also observed that a reasonable converged results are obtained by the proposed methodology when $n \geq 9$and $m \geq 65$. The effects of location of truncated boundary on accuracy and convergence of results are investigated in Fig. 4. It can be seen that the accuracy and convergence of the solutions are mainly dictated by the choice of location of truncated boundary. Note that, when the truncated boundary is not located far enough, inaccurate and oscillatory results can be obtained for the responses of the fluid. In Fig. 5, the results of present mixed methodology are compared with the exact solution results of Lee and Tsai [9]. An excellent agreement can be seen.

Next, we evaluated the responses of the fluid-structure system subjected to 1940 EI Centro earthquake (Fig. 6). The results are shown in Fig. 7. The exact solution results of Lee and Tsai [9] are also shown for comparison purposes. It can be seen that the results generated by the proposed method agree well with those of [9].

B. Response of Variable Thickness Dam-Structures of Equal Weight Subjected to Ground Motion

In this study we are interested to analyze the dynamic behavior of variable thickness dam-structures of equal weight subjected to ground motion. Fig. 8 shows some linearly varying thickness dam-structures with equal weight. For these cases, the thickness of the dam varies in the z-direction in the following linear fashion

$$h(z) = h_u \left(\frac{2(T_r - 1)}{(T_r + 1)} z + \frac{2}{(T_r + 1)} \right) \tag{70}$$

where h_u is the thickness of a uniform cross-section dam (see Fig. 8) and T_r is the thickness ratio defined as:

$$T_r = \frac{h(z=L)}{h(z=0)}, \qquad 0 \leq T_r \leq 1 \tag{71}$$

Note that, in dam-structures, the thickness of the dam at $z = L$ is always equal or smaller than that at $z = 0$. For this reason, the thickness ratio (T_r) is always smaller or equal to unity (i.e., $T_r \leq 1$). It can also be easily verified that, for every thickness ratio, the volume of dams that their thickness obey (70) is equal to $V_u = A_u L = b h_u L$ (where b is the width of the dam cross-section and assumed here to be unity).

To study the effect of the thickness ratio on the dynamic behavior of the fluid-structure system, the dimensions and material properties of the fluid and structure are considered as follows. Depth of the fluid domain $L = 100\ m$, acoustic wave speed in water $C = 1438.656\ \mathrm{m/s}$, mass density of the water $\rho_f = 1000\ \mathrm{Kg/m^3}$, modulus of elasticity of the structure $E = 3 \times 10^{10}\ \mathrm{N/m^2}$, mass density of the structure $\rho_s = 2320\ \mathrm{Kg/m^3}$, thickness of the uniform cross-section structure $h_u = 10$ m and width of the structure $b = 1$ m.

Fig. 9 shows the variation of natural frequencies ($\Omega_i,\ i = 1,2,3,4,5$) of variable thickness dams versus thickness ratio (T_r). It can be seen from Fig. 9 that the lower order natural frequencies decrease as the thickness ratio increases. This means when the system is subjected to low frequency excitation, the use of variable thickness structures (say tapered structure) can improve the dynamical behavior of the system significantly. However, the higher order natural frequencies do not show the same trend. It is seen that there is a range for the thickness ratio where the higher order natural frequencies increase as the thickness ratio increases (here, this range is approximately $0 \leq T_r \leq 0.4$ as it can be seen from Fig. 9). This means, when the structure is subjected to high frequency excitation and the thickness ratio is in the range $0 \leq T_r \leq 0.4$, the response of the structure may not be highly influenced by the variation in thickness ratio. For this case, it is also possiblethat the response of the variable thickness structure decreases as the thickness ratio increases.

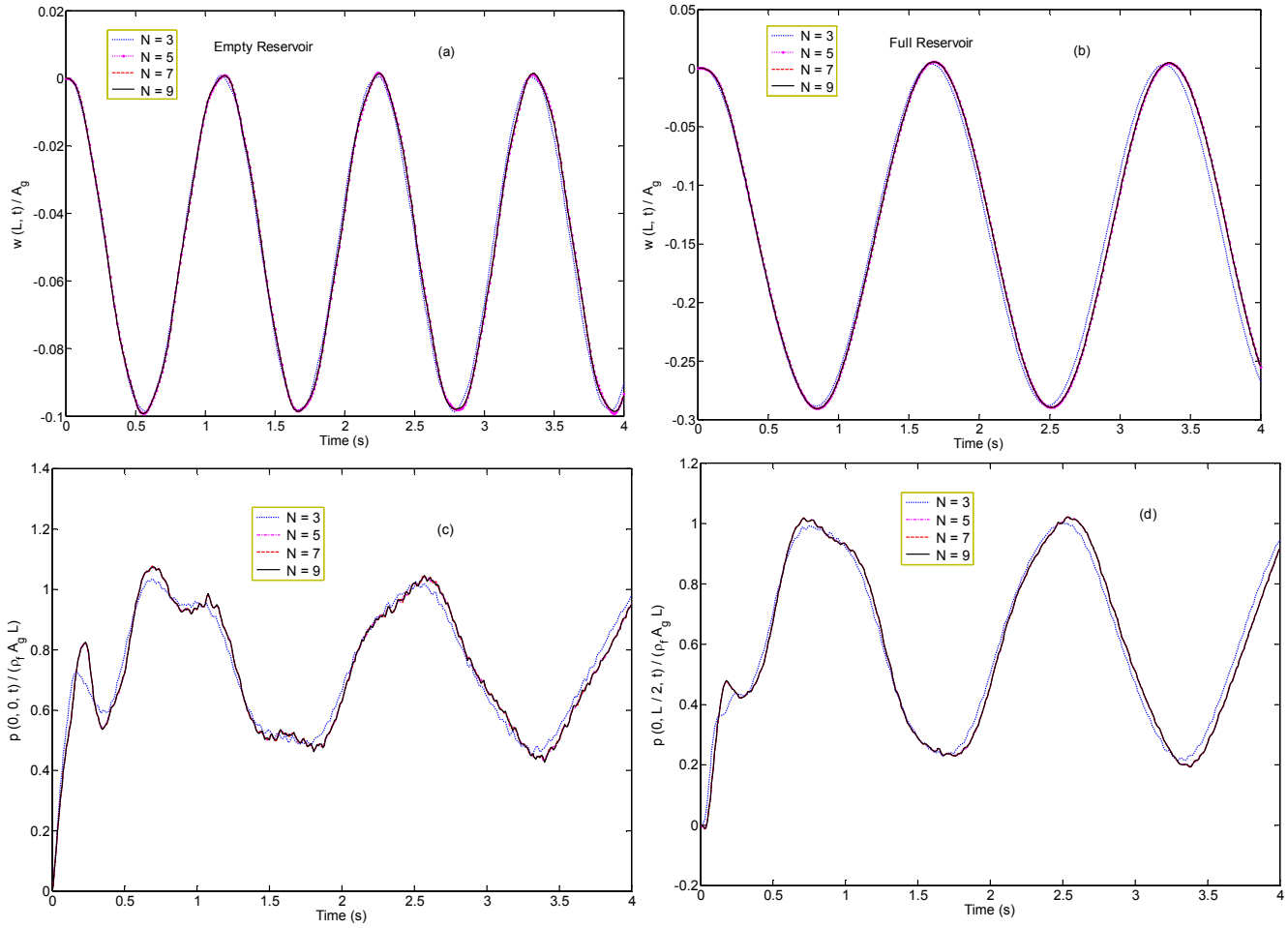

Fig. 2 Convergence of solutions with respect to the order of interpolation functions (N) for the case of ramp acceleration: (a) displacement at top of structure in empty reservoir case, (b) displacement at top of structure in full reservoir case, (c) hydrodynamic pressure at bottom of reservoir, and (d) hydrodynamic pressure at middle of reservoir

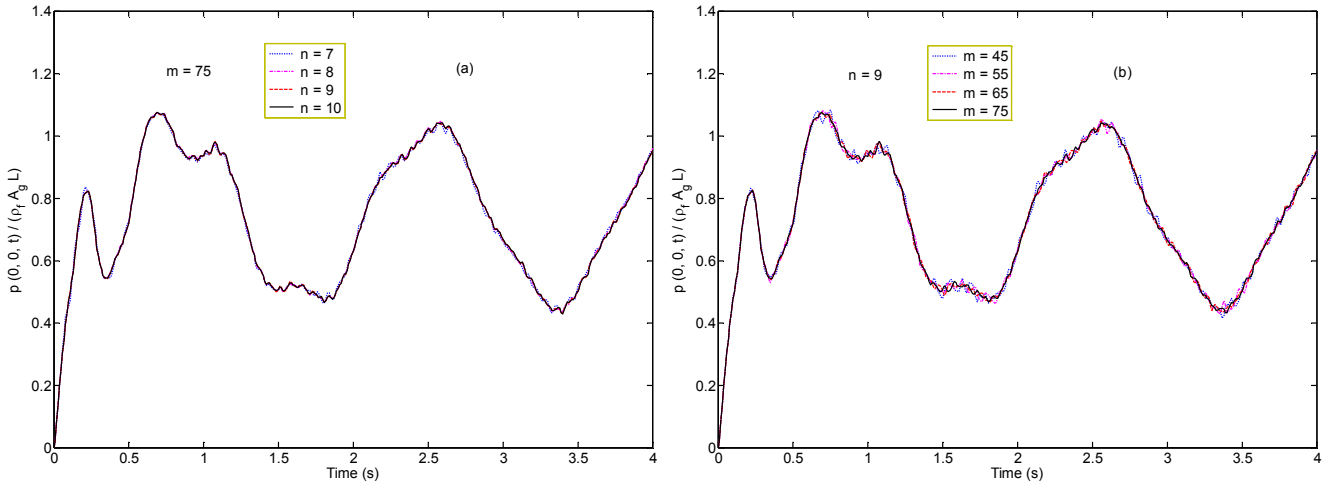

Fig. 3 Convergence of hydrodynamic pressure at bottom of reservoir in the case of ramp acceleration with $N = 5$: (a) convergence with respect to the number of DQM sampling points in the z-direction, n, and (b)convergence with respect to the number of DQM sampling points in the x-direction, m

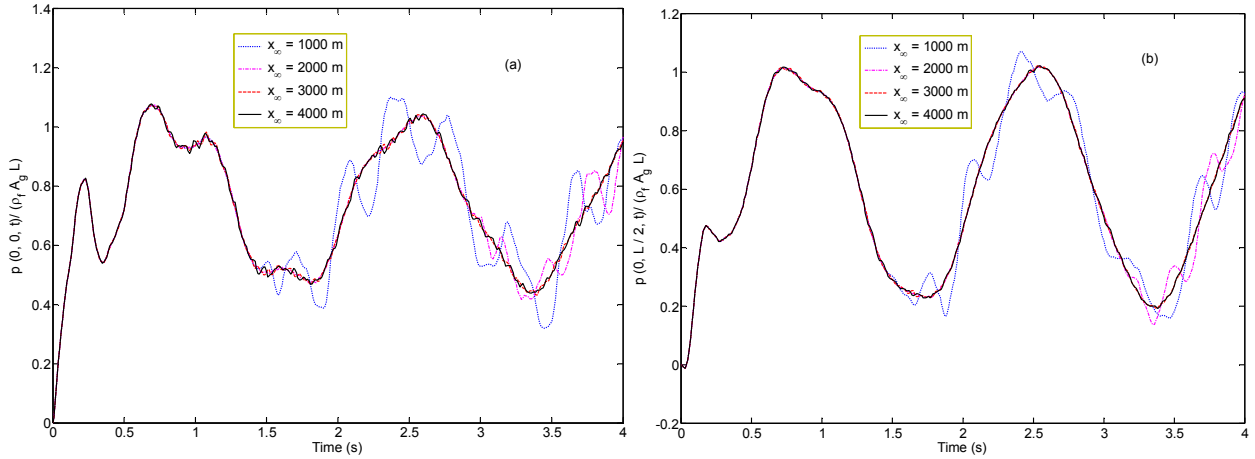

Fig. 4 Effect of location of truncated boundary on responses of fluid subjected to ramp acceleration: (a) hydrodynamic pressure at bottom of reservoir, and (b) hydrodynamic pressure at middle of reservoir

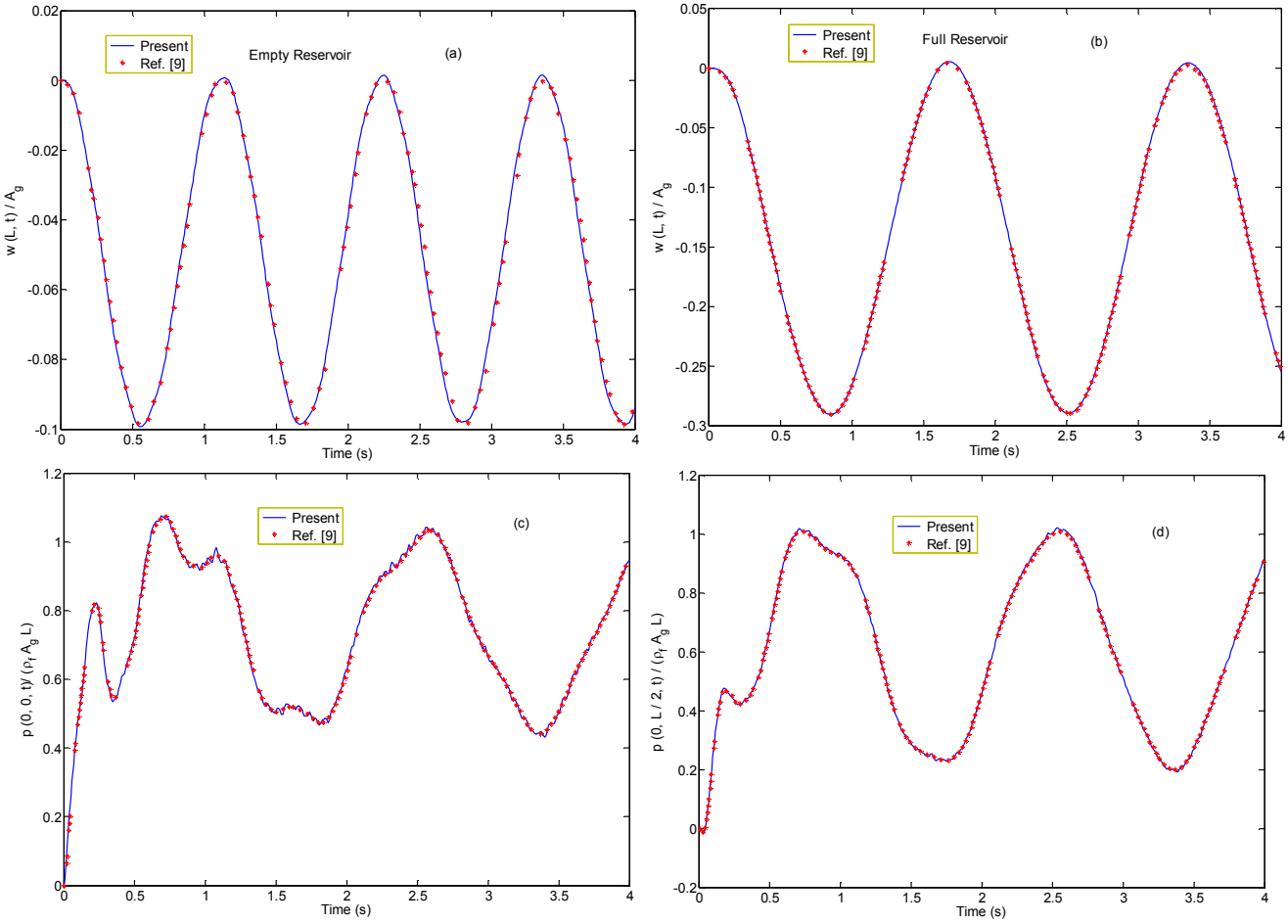

Fig. 5 Comparison of results of present method with exact solution results of [9] for responses of dam-reservoir system subjected to ramp acceleration: (a) displacement at top of structure in empty reservoir case, (b) displacement at top of structure in full reservoir case, (c) hydrodynamic pressure at bottom of reservoir, and (d) hydrodynamic pressure at middle of reservoir

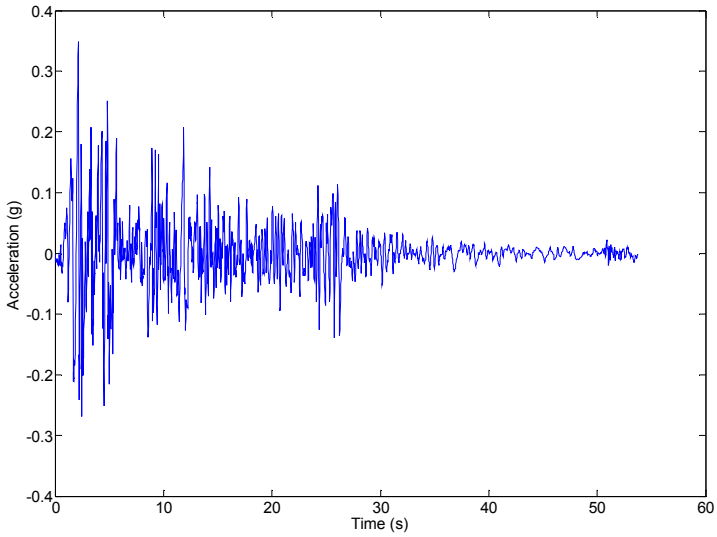

Fig. 6 Ground acceleration due to EI Centro earthquake 1940

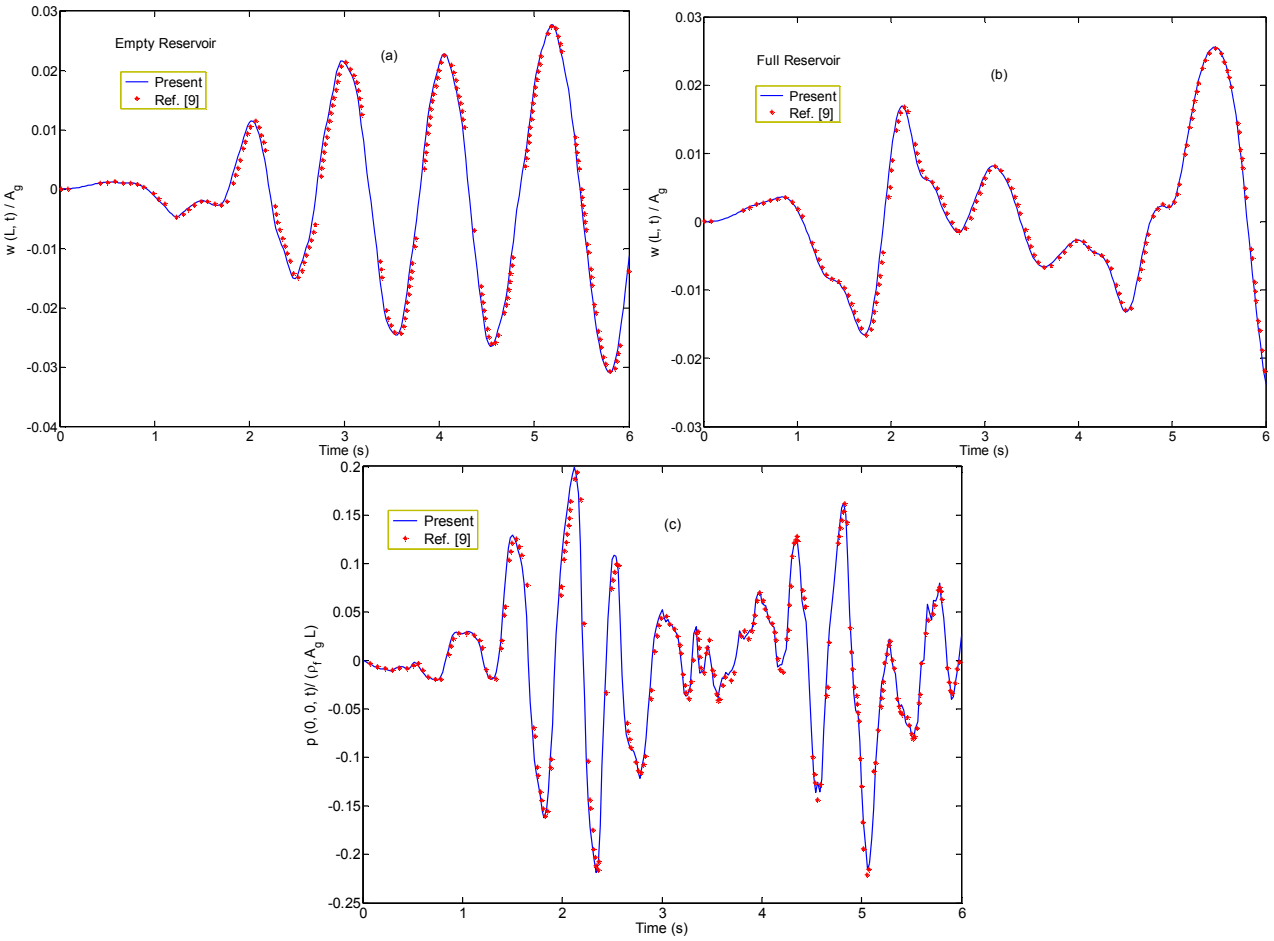

Fig. 7 Comparison of Results of present method with exact solution results of [9] for responses of dam-reservoir system subjected to 1940 EI Centro ground motion: (a) displacement at top of structure in empty reservoir case, (b) displacement at top of structure in full reservoir case, and (c) hydrodynamic pressure at bottom of reservoir

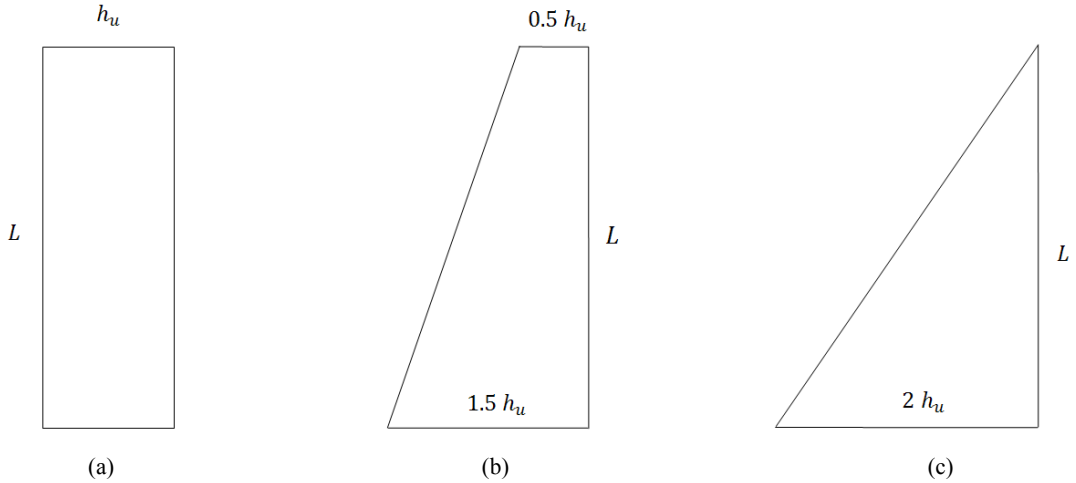

Fig. 8 Variable thickness dam-structures of equal weight with different thickness ratios: (a) T_r= 1, (b) T_r= 1/3, (c)T_r= 0

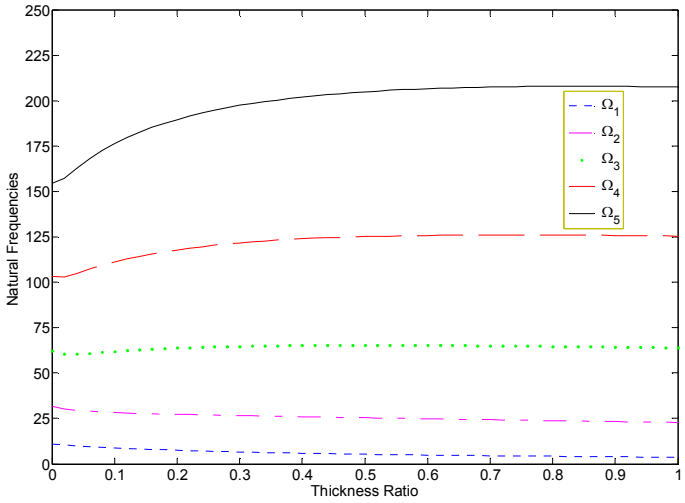

Fig. 9 Variation of natural frequencies of variable thickness dams versus thickness ratio

In Fig. 10 the convergence of solutions for the response of variable thickness dam is investigated for different values of *N*. Comparing these results with those of Section VI *A* one may conclude that larger values of *N* should be used in the algorithm for the case of variable thickness dams. In Figs. 11 and 12 the effect of thickness ratio on the dynamic response of variable thickness dams subjected to ramp acceleration and 1940 EI Centro earthquake is investigated. It can be seen that in the case of ramp acceleration the response of the structure is highly influenced by the variation of the thickness ratio. The reason for this is that the ramp acceleration may be viewed as a low-frequency excitation. Thus, the response of the structure decreases considerably as the thickness ratio decreases. However, in the case of 1940 EI Centro earthquake, the response of the structure is not highly influenced by the variation of thickness ratio. This is a reasonable result, because the 1940 EI Centro earthquake may be viewed as a high frequency excitation. Thus, the response of the structure may increase or decrease by decreasing the thickness ratio. Note that, in all cases, the response of the variable thickness dam is smaller than that of the uniform dam.

VII. Conclusion

A simple and accurate mixed Galerkin-DQ formulation is proposed for the transient analysis of the dam-reservoir interaction. The Galerkin method is applied for the structural part, whereas the DQM is used for the fluid domain. The proposed mixed method combines the simplicity of the Galerkin method and high accuracy and efficiency of the DQM. Its reliability, accuracy and efficiency are demonstrated by comparing the calculated results with those available in the literature. It is shown that highly accurate results can be obtained using a small number of Galerkin terms and DQM sampling points. The technique presented in this investigation is general and can be used to solve various fluid-structure interaction problems.

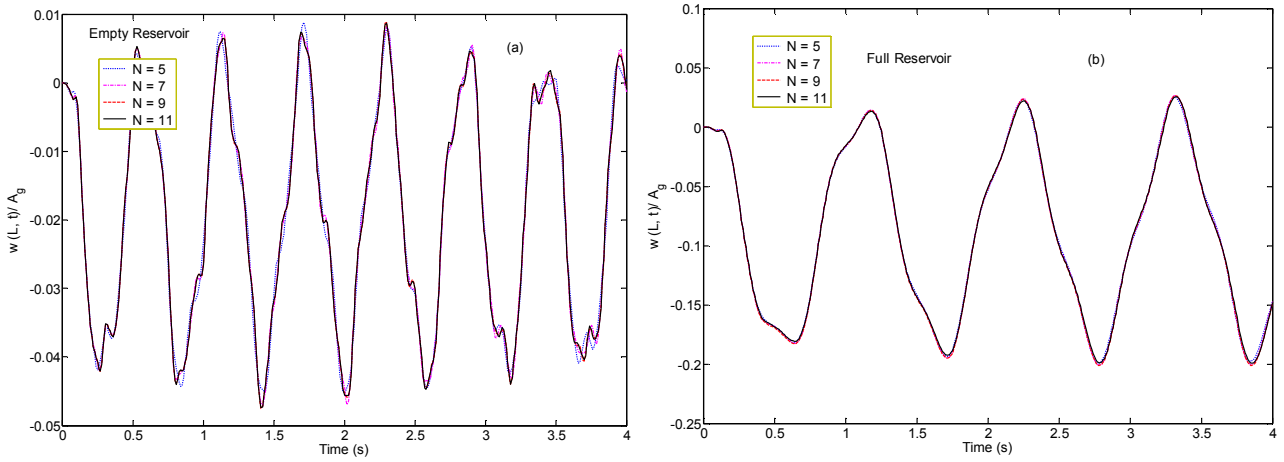

Fig. 10 Convergence of response of the variable thickness structure subjected to ramp acceleration with respect to the order of interpolation functions *N* for $T_r = 0$: (a) displacement at top of structure in empty reservoir case, (b) displacement at top of structure in full reservoir case

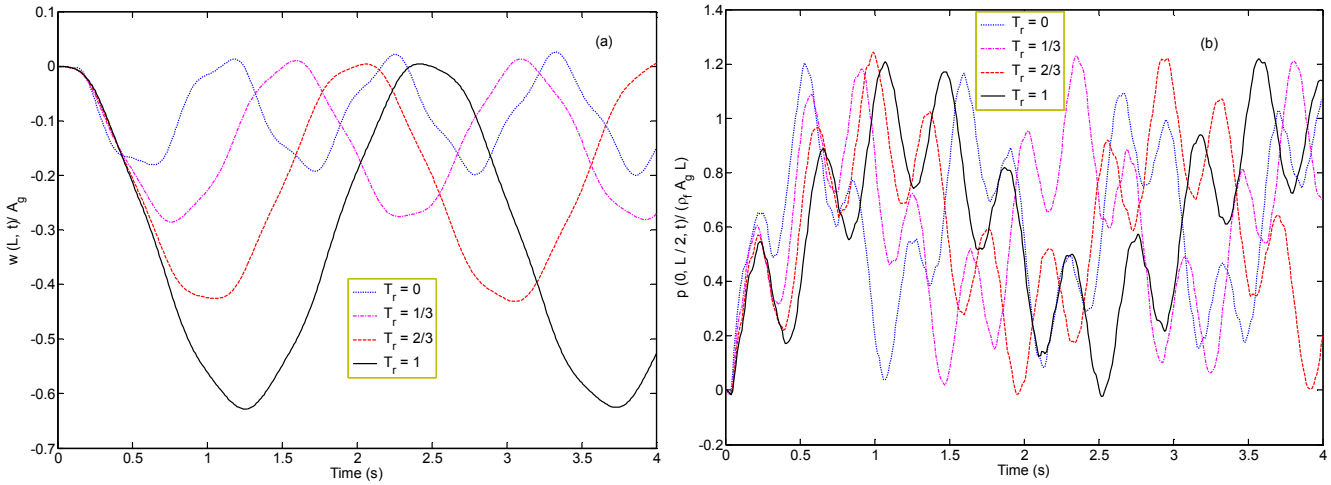

Fig. 11 Effect of thickness ratio on the responses of the dam-reservoir system subjected to ramp acceleration: (a) displacement at top of structure in full reservoir case, and (b) hydrodynamic pressure at middle of reservoir

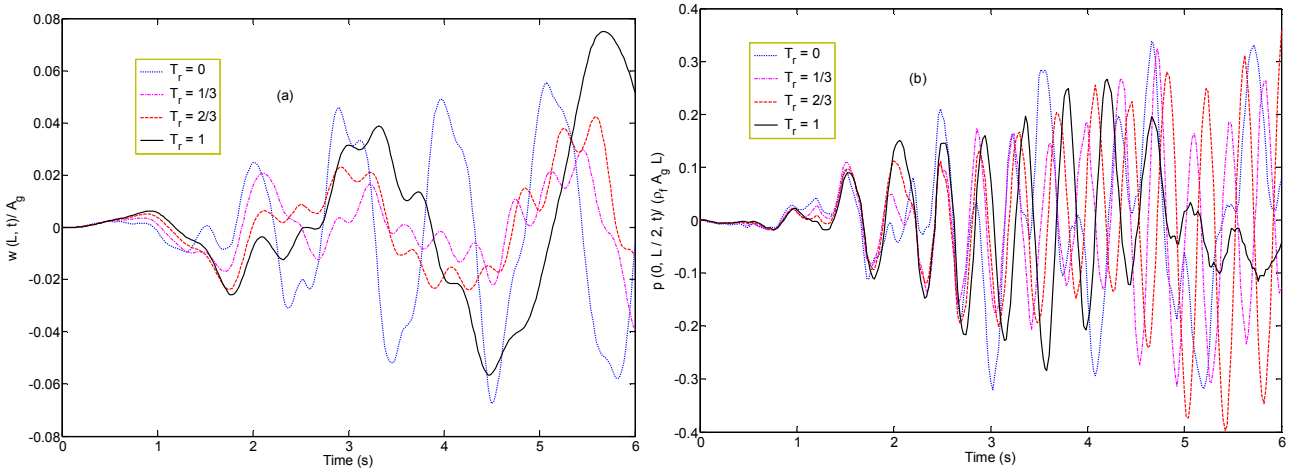

Fig. 12 Effect of thickness ratio on the responses of the dam-reservoir system subjected to1940 EI Centro ground motion: (a) displacement at top of structure in full reservoir case, and (b) hydrodynamic pressure at middle of reservoir

REFERENCES

[1] H. M. Westergaard, "Water pressures on dams during earthquakes," *Trans. ASCE*, vol. 98, pp. 418–472, 1933.
[2] A. K. Chopra, "Hydrodynamic pressures on dams during earthquakes," *ASCE J. Eng. Mech.*, vol. 93, no. 6, pp. 205-223, 1967.
[3] A. T. Chwang, "Hydrodynamic pressures on sloping dam during earthquakes-Part 2: Exact theory," *J. Fluid Mech*., vol. 87, pp. 343-348, 1978.
[4] P.L.-F. Liu, "Hydrodynamic pressures on rigid dams during earthquakes," *J. Fluid Mech*., vol. 165, pp. 131-145, 1986.
[5] D. Maity, and S. K. Bhattacharyya, "A parametric study on fluid-structure interaction problems," *J. Sound. Vib*., vol. 263, pp. 917-935, 2003.
[6] S. S. Saini, P. Bettess, and O. C. Zienkiewicz, "Coupled hydrodynamic response of concrete gravity dams using finite and infinite elements," *Earthquake Eng. Struct. Dyn*., vol. 6, pp. 363–374, 1978.
[7] C. S. Tsai, and G .C. Lee, "Arch dam-fluid interactions: by FEM-BEM and substructure concept," *Int. J. Numer. Methods Eng*., vol. 24, pp. 2367-2388, 1987.
[8] V. Lotfi, J.M. Roesset, and J.L. Tassoulas, "A technique for the analysis of the response of dams to earthquakes," *Earthquake Eng. Struct. Dyn*., vol. 15, pp. 463–490, 1987.
[9] G.C.Lee, and C.S.Tsai, "Time domain analysis of dam-reservoir system. I: Exact solution,"*ASCE J. Eng. Mech*., vol. 117, pp. 1990-2006, 1991.
[10] C.S.Tsai, G.C. Lee, and R.L.Ketter, "Solution of the dam-reservoir interaction problem using a combination of FEM, BEM with particular integrals, modal analysis, and substructuring," *Eng. Anal. Bound. Elem.*, vol. 9, pp. 219-232, 1992.
[11] T. Touhei, and T.Ohmachi, "A FE-BE method for dynamic analysis of dam-foundation-reservoir systems in the time domain," *Earthquake Eng. Struct. Dyn*.,vol. 22, no. 3, pp. 195–209, 1993.
[12] M.Ghaemian, and A.Ghobarah, "Staggered solution schemes for dam-reservoir interaction," *J. Fluids Struct*., vol. 12, pp. 933-948, 1998.
[13] S. Küçükarslan, and S.B.Coşkun, "Transient dynamic analysis of dam-reservoir interaction by coupling DRBEM and FEM,"*Eng. Comput.*, vol. 21, no. 7, pp. 692-707, 2004.
[14] M.Akköse, S. Adanur, A.Bayraktar, and A.A.Dumanoğlu, "Stochastic seismic response of Keban dam by the finite element method," *Appl. Math. Comput.*,vol. 184, no. 2, pp. 704-714, 2007.
[15] S. C. Fan, and S.M.Li, "Boundary finite-element method coupling finite-element method for steady-state analysis of dam-reservoir systems,"*ASCE J. Eng. Mech*., vol. 134, no.2, pp. 133–142, 2008.
[16] P. M.Mohammadi, A. Noorzad, M. Rahimian, and B.Omidvar, "The Effect of interaction between reservoir and multi-layer foundation on the dynamic response of a typical arch dam (Karaj dam) to "P" and "S" waves,"*Arabian J. Sci. Eng*., vol. 34, no. 1B, pp. 91-106,2009.
[17] N.Bouaanani, and F.Y.Lu, "Assessment of potential-based fluid finite elements for seismic analysis of dam-reservoir systems," *Comput. Struct.*,vol. 87, pp. 206–224, 2009.
[18] A.Seghir, A.Tahakourt, and G.Bonnet, "Coupling FEM and symmetric BEM for dynamic interaction of dam–reservoir systems,"*Eng. Anal. Bound. Elem*., vol. 33, pp. 1201–1210, 2009.
[19] M.R.Koohkan, R. Attarnejad, and M.Nasseri, "Time domain analysis of dam-reservoir interaction using coupled differential quadrature and finite difference methods,"*Eng. Comput*., vol. 27, no. 2, pp. 280-294, 2010.
[20] A.AftabiSani, and V.Lotfi, "Dynamic analysis of concrete arch dams by ideal-coupled modal approach," *Eng. Struct*., vol. 32, pp. 1377–1383, 2010.
[21] N.Bouaanani, and C. Perrault, "Practical formulas for frequency domain analysis of earthquake-induced dam-reservoir interaction," *ASCE J. Eng. Mech*., vol. 136, pp. 107–119, 2010.
[22] M.Mirzayee, N. Khaji, and M.T.Ahmadi, "A hybrid distinct element–boundary element approach for seismic analysis of cracked concrete gravity dam–reservoir systems," *Soil Dyn. Earthquake Eng*., vol. 31, pp. 1347–1356, 2011.
[23] X.Wang, F. Jin, S.Prempramote, and C.Song, "Time-domain analysis of gravity dam-reservoir interaction using high-order doubly asymptotic open boundary,"*Comput. Struct*.,vol. 89, no. 7-8, pp. 668–680, 2011.
[24] A.Samii, and V.Lotfi, "Application of H–W boundary condition in dam–reservoir interaction problem," *Finite Elem. Anal. Des*.,vol. 50, pp. 86–97, 2012.
[25] C.W.Bert, and M.Malik, "Differential quadrature method in computational mechanics: A review," *ASME Appl. Mech. Rev*., vol. 49, pp. 1–28, 1996.
[26] S.M.R.Khalili, A.A.Jafari, and S.A.Eftekhari, "A mixed Ritz-DQ method for forced vibration of functionally graded beams carrying moving loads," *Compos. Struct*.,vol. 92, no. 10, pp. 2497–2511,2010.
[27] A.A.Jafari, and S.A.Eftekhari, "An efficient mixed methodology for free vibration and buckling analysis of orthotropic rectangular plates,"*Appl. Math. Comput*., vol. 218, pp. 2670–2692,2011.
[28] S.A.Eftekhari, and A.A.Jafari, "Coupling Ritz method and triangular quadrature rule for moving mass problem,"*ASME J. Appl. Mech*., vol. 79, no.2, 021018, 2012.
[29] S.A. Eftekhari, and A.A. Jafari, "Vibration of an initially stressed rectangular plate due to an accelerated traveling mass," *Sci. Iran. A*, vol. 19, no.5,pp. 1195–1213,2012.
[30] S.A. Eftekhari, A.A. Jafari, "Modified mixed Ritz-DQ formulation for free vibration of thick rectangular and skew plates with general boundary conditions," Appl. Math. Model. vol. 37, pp. 7398–7426, 2013.
[31] S.A. Eftekhari, A.A. Jafari, "A simple and accurate mixed FE-DQ formulation for free vibration of rectangular and skew Mindlin plates with general boundary conditions," Meccanica vol. 48, pp. 1139–1160, 2013.
[32] C. Shu, Differential Quadrature and Its Application in Engineering. New York: Springer-Verlag, 2000.
[33] K.J. Bathe, and E.L. Wilson, Numerical Methods in Finite Element Analysis. NJ: Prentic-Hall, Englewood Cliffs, 1976.

Seyyed Aboozar Eftekhari was born in Karaj, Iran, in 1980. He received a BS degree in Mechanical Engineering from Sharif University of Technology, Tehran, Iran, in 2003, an MS degree in Mechanical Engineering from Shiraz University, Shiraz, Iran, in 2006, and a PhD degree in Mechanical Engineering from K. N. Toosi University of Technology, Tehran, Iran, in 2013.

He is currently a member of Young Researchers and Elite Club, Karaj Branch, Islamic Azad University, Karaj, Iran. His research interests include applied mathematics, time integration schemes, vibration of continuous systems, and fluid-structure interaction. He has published over 20 research papers on related subjects, including the study ofthe behavior of beams and plates under moving loads, mathematical modeling of vibration problem of beams and plates, and numerical solution of nonlinear differential equations in engineering and applied sciences.